Indian Journal of Engineering & Materials Sciences
Vol. 23, February 2016, pp. 20-26

Synthesis, microstructure and mechanical properties of Al-Si-Mg alloy hybrid (zircon + alumina) composite

T Satish Kumar[a], R Subramanian[a], S Shalini[b], J Anburaj[a] & P C Angelo[c]*

[a]Department of Metallurgical Engineering, PSG College of Technology, Coimbatore 641 004, India

[b]Department of Physics, PSG College of Technology, Coimbatore 641 004, India

[c]Metal Testing & Research Centre, PSG College of Technology, Coimbatore-641004, India

Received 2 February 2015; accepted 7 December 2015

In the present work, a detailed study of zircon and alumina reinforcement in to the matrix of Al-Si-Mg alloy on the microstructure and wear behavior has been carried out. To study the effect of reinforcement on the wear behaviour of these composites, the alloy is reinforced with different amounts of zircon and alumina particles limiting to the total 15 wt%. The microstructure of these hybrid composites reveal uniform distribution of the reinforced particles. Composites are found to exhibit better hardness and wear resistance compared to base alloy. Among the different composites, the one reinforced with 3.75 wt% of zircon and 11.25 wt% of alumina particles (composite B) is found to be the best combination exhibiting high hardness and low wear rate at a test load of 15 N. SEM analysis of worn surface of hybrid composites shows no evidence of plastic deformation of matrix phase. Abrasive wear mechanism and particle pull out is the common feature observed from all the composites.

Keywords: Metal-matrix composite, Hardness, Abrasion, Wear, Fracture

Aluminum matrix hybrid composites (Al MHCs) are considered as a good choice of study because of their excellent properties such as high strength, low density, easy workability, good corrosion and wear resistance[1-4]. Hence, Al MHCs are widely preferred in different fields ranging from automotive industries to aerospace applications[2,3]. In recent days, attempts are being made to develop Al MHCs with different reinforcements such as SiC, Al_2O_3, zircon, graphite or a combination of these reinforcements[2,5-7]. Das ***et al***.[2] investigated the abrasive wear behavior of Al MHCs synthesized by stir casting route with incorporation of silicon carbide particles and zircon as reinforcements. Wear resistance of aluminium alloy was found to be dependent on the amount, particle size and type of reinforcement. Ploughing of the surface by abrading silicon carbide particles was reported to be the main wear mechanism in these Al MHCs. Similarly, zircon sand and graphite particulates were used as reinforcement by Gopi ***et al***.[5] A considerable improvement in the hardness and wear resistance was reported for heat treated composites compared to as-cast composites.

Effect of high temperature on wear behavior of aluminium alloy was studied by Sharma ***et al***.[6] According to the reports, a combination of zircon sand and silicon carbide particle in a ratio of 1:3 as reinforcement in the composite exhibited better wear resistance compared to other combinations. The tribological behavior of self-lubricating graphite/ SiC/Al hybrid composites as a function of graphite content was studied by Guo ***et al***.[7] The wear rate was found to increase up to 5% of graphite addition and then lowered at 8% of graphite.

Wang ***et al***.[8] investigated the room temperature sliding wear behavior of Al_2O_3 and SiC particulate reinforced Al MHC under both dry as well as lubricated conditions. Under dry sliding condition, the wear behaviour of the hybrid composites was reported to be better than composites incorporated with fibres exhibiting random orientation. On the contrary, under lubricated conditions, wear behaviour of the hybrid composites was reported to be better on incorporating the alloy with fibers possessing normal orientation. Room temperature sliding wear behavior of Al MHC's was investigated by Ahlatci ***et al***.[9] The role of magnesium addition along with SiC and Al_2O_3 particles on dry sliding wear behavior of Al MHC's was investigated. The wear resistance of the composites was found to increase with increasing addition of magnesium. Song ***et al***.[10] successfully fabricated Al MHC by squeeze casting method

*Corresponding author (E-mail: angelopsg@gmail.com)

with Al_2O_3 and C as hybrid reinforcements. Wear resistance of Al/Al_2O_3 and $Al/Al_2O_3/C$ composites was found to improve remarkably with the addition of reinforcements compared to the matrix alloy. Wear resistance of hybrid composite reinforced with alumina and carbon fiber was better than that of composite reinforced with alumina alone.

In the present investigation, hybrid composites were fabricated by reinforcing with different amounts of zircon sand and alumina particle in an Al-Si-Mg alloy prepared by stir-casting route. This work mainly aims to investigate the effect of the amount of reinforcement on the wear properties of the synthesized hybrid composites. The wear behavior of the hybrid composites was evaluated by using a pin-on-disc wear and friction monitor. The hardness of the composites was measured by Brinell harness tester. The presence and distribution of the reinforced particles was confirmed using optical microscopy. The microstructure of the worn surface was examined by scanning electron microscopy (SEM) to understand the wear mechanism operating during wear test.

Experimental Procedure

Materials

Compositional analysis of Al-Si-Mg alloy used in the present study was carried out by optical emission spectroscopy and is summarized in Table 1.

Synthesis

500 g of Al-Si-Mg alloy was taken in a clay graphite crucible and melted at 750ºC. Commercially pure zircon (99.5%) particles of size ranging from 105-125 µm and alumina (99.9%) particles of size 88-105 µm selected as reinforcements for the study, were preheated at 200ºC for 2 h to eliminate moisture content of the particles before adding to the alloy melt. A stirrer was then lowered into the crucible and the stirrer speed was gradually raised to 600 rpm. A vortex was created in the melt due to the action of stirrer and then the preheated particles were added into the melt at a rate of 10 g/min. Alumina particles were added first into the melt followed by the addition of zircon particles. Then the melt was stirred for 10 min to ensure uniform distribution of particles throughout the matrix. The melt from the graphite crucible was then poured into small metal moulds.

Table 1 – Chemical composition of the Al-Si-Mg alloy

Al-Si-Mg alloy	Si	Fe	Cu	Mn	Mg	Zn	Ni	Al
wt %	7.5	0.3	0.2	0.3	0.6	0.1	0.1	90.9

Based on previous studies[3,11-14], it was observed that 15 wt% of reinforcement addition into the alloy exhibited better property. Hence, the % reinforcement in the present study was restricted to 15 wt%. In order to study the effect of the amount of reinforcement particles on the properties of the hybrid composite, five different composites containing a total of 15 wt% of zircon and alumina reinforcement as shown in Table 2 were synthesized.

Dry sliding wear behaviour of the alloy and the synthesized hybrid composites were carried out at room temperature using a pin-on-disc wear and friction monitor (Model TR-20, Ducom, Bangalore). Cylindrical samples of length 30 mm and diameter 10 mm were tested against a hardened EN32 steel disc having a hardness of 65 HRC. This procedure was repeated four times and the wear rate was calculated by taking the average of the wear test results. Wear rate for the pin was calculated using the Eq. (1)[2,4] as per ASTM standard G99.

$$\boldsymbol{W}(\boldsymbol{mm}^3\boldsymbol{m}^{-1}) = \frac{\boldsymbol{M}(\boldsymbol{g}) / \boldsymbol{D}(\boldsymbol{g}/\boldsymbol{mm}^{-3})}{\text{sliding distance}\,(\boldsymbol{m})} \quad \ldots (1)$$

where $\boldsymbol{M}$ is mass loss during abrasive wear and $\boldsymbol{D}$ isdensity of the respective composite.

Hardness of Al-Si-Mg alloy as well as the composites was measured by Brinell hardness tester using 10 mm steel ball indenter. A load of 500 kg was used to determine the hardness of both the alloy and the composites. The hardness values were plotted by taking an average of 4 readings for each sample. Microstructural analysis of the alloy and the composites was studied by mechanically polishing and etching the samples by Keller's reagent. Microstructure of these etched samples was studied by using both optical microscopy (Eclipse MA-100, Nikon) (Carl Zeiss) and scanning electron microscope (JEOL, JSM-6510LV).

X-ray diffraction analysis was carried out on the as-cast composites using (XRD 6000, Shimadzu) X-ray diffractometer with Cu Kα radiation (λ=1.5409 Å). Each of the samples was scanned with 2θ values

Table 2 – Composition of the composites containing zircon and alumina particles made by stir casting

Sample name	wt% of reinforcement
A	15 % Al_2O_3
B	11.25 % Al_2O_3 + 3.75 % $ZrSiO_4$
C	7.5 % Al_2O_3 + 7.5 % $ZrSiO_4$
D	3.75 % Al_2O_3 + 11.25 % $ZrSiO_4$
E	15 % $ZrSiO_4$

ranging from 10° to 80°. The angles of the characteristic peaks of different phases were measured from the plot and indexed by using JCPDF data.

Results and Discussion

Microstructural analysis

The optical micrograph of the as-cast monolithic Al-Si-Mg alloy shows the presence silicon particles in the interdendritic region of coarse α-aluminium matrix as shown in Fig. 1 (a).

The optical micrographs of the composites are shown in Fig. 1 (b-f). Compared to the as-cast monolithic Al-Si-Mg alloy (Fig. 1(a)), the microstructure of all the composites shows modification in the α-aluminium dendrites. This can be due to factors such as dentritic fragmentation, restriction of particles by dendritic growth and higher temperature difference between the particle and the melt[15-18]. The fragmentation in dendritic structure is due to the shearing of initial dendritic arms by the stirring action. The ceramic reinforcement particles provide site for nucleation of melt as temperature difference between particle and the melt is higher[19-21].

The reinforcement particles in all the composites were found to be more or less uniformly distributed in

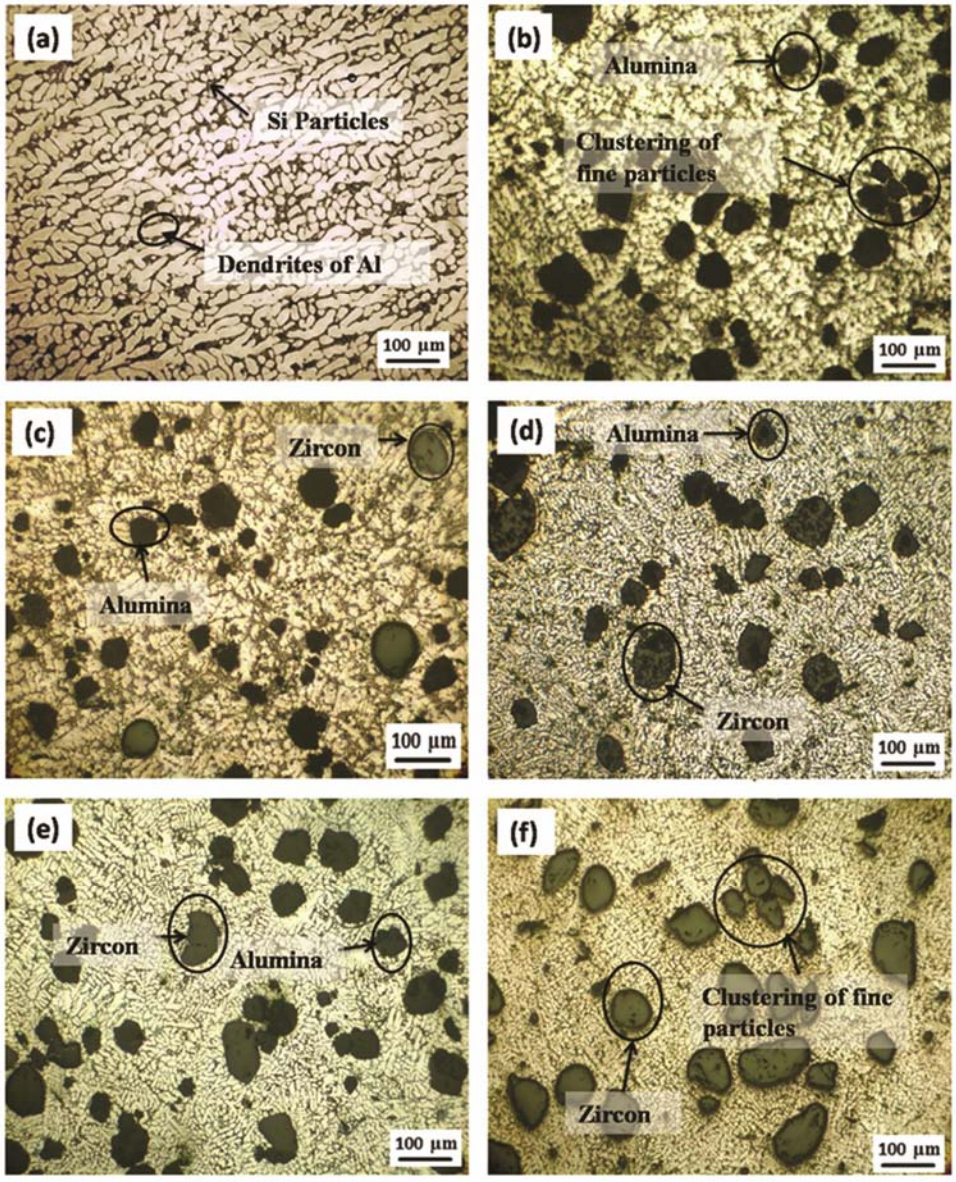

Fig. 1 – Optical micrograph of composites at 100X (a) as-cast Al-Si-Mg alloy (b) Composite A (c) Composite B (d) Composite C (e) Composite D (f) Composite E

the matrix with clustering of particles at few places as in the case of composite A and composite E. Refinement in dendritic structure of the matrix with uniformly distributed reinforcement particles will improve the hardness of the composite. Moreover, porosity is not observed during optical examination, although clustering of particles is observed at a few places in the composite.

SEM images show the morphology of alumina particle (Fig. 2 (a)) and zircon particle (Fig. 2 (b)) reinforced composite at higher magnification. The morphology of zircon particle appears rough and irregular compared to alumina particles thus exhibiting good bonding with matrix.

XRD analysis

X-ray diffraction analysis was carried out to confirm the phases revealed by metallography. X-ray diffraction pattern for all the composites (A-E) is shown in Fig. 3. The pattern revealed the peaks of Al, Si, $ZrSiO_4$ and Al_2O_3 confirming the presence of $ZrSiO_4$ and Al_2O_3 in the synthesized composite.

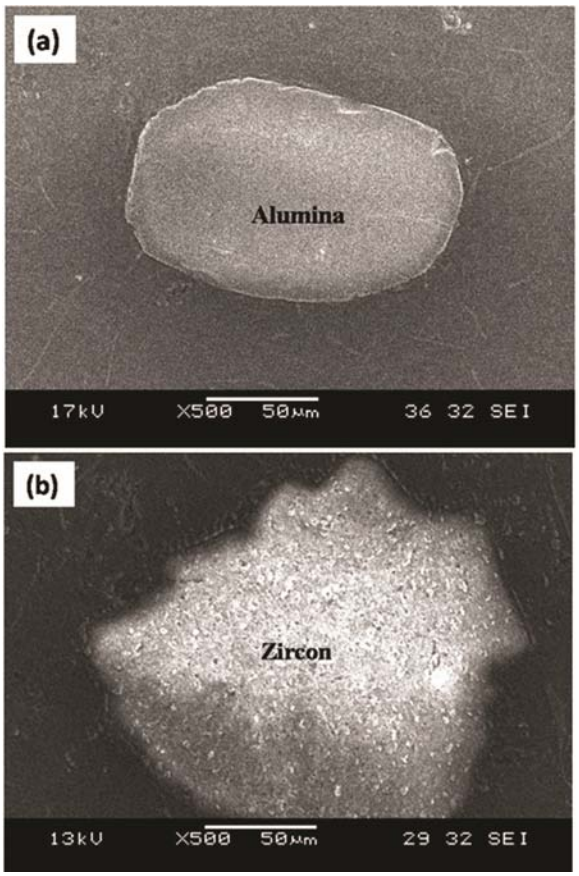

Fig. 2 – SEM images of (a) alumina particle (b) zircon particle

Hardness

Figure 4 shows the hardness values of the as-cast alloy and composites. All the composites were found to possess higher hardness than the base alloy (55 BHN). From the graph, it is clear that the composites exhibit higher hardness than unreinforced alloy. According to Dunand ***et al***.[14], a large difference in thermal expansion coefficient between the matrix and the reinforcement leads to the generation of higher dislocation density in the matrix of the composite. This increased dislocation density of Al alloy matrix leads to an increase in hardness of the composite compared to that of unreinforced alloy. Reinforcement of particles into any matrix will generally act as nucleation sites and refine the matrix grain size. Refinement of grain size tends to improve the hardness of the composite[12]. In this case, addition of zircon and alumina refines α-aluminium dendrites in the matrix leading to increase in hardness of the composite.

In comparison with all other composites, composite B exhibits higher hardness. This is due to the combination of higher proportion of harder alumina particles with good interfacial bonding rendered by

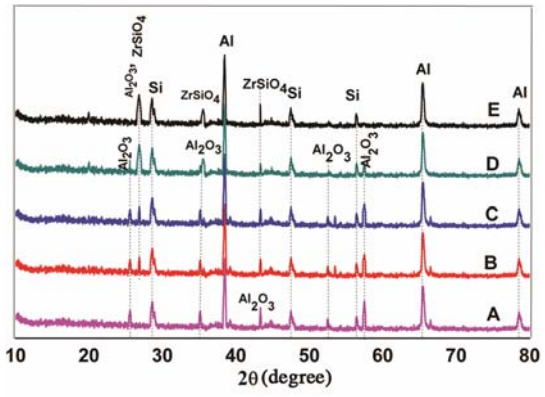

Fig. 3 – X-ray diffraction patterns for all the composites

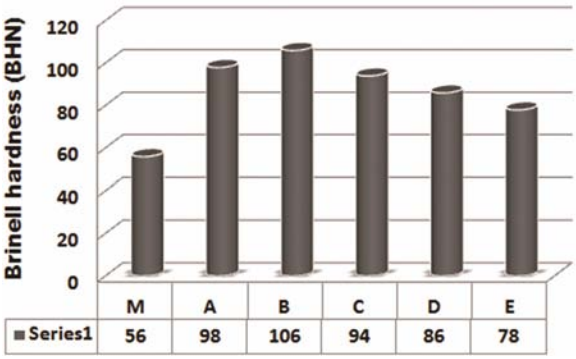

Fig. 4 – Hardness of base alloy (M) and composites (A-E)

rough and irregular shaped zircon particles. In the case of composite A, in spite of the presence of higher proportion of harder alumina particles, the hardness of the composite is found to be lesser than that of composite B. This can be attributed to the clustering of particles at few places in the matrix as revealed by the microstructure. This clustering acts as weak centers and is the potential sites for damage accumulation which decreases the hardness of the composite. Similar results have been reported by employing SiC as reinforcement into 8090 Al alloy by Bauri ***et al***.[12] In the case of composite C and composite D, the hardness is found to be less due to the presence of lesser proportion of harder alumina particles. Finally as composite E contains only zircon particles that can render good bonding with the matrix; the hardness of the composite is found to be lesser than composite A due to the absence of harder alumina particles.

Wear characteristics

Abrasive wear behavior of the Al-Si-Mg alloy (M) and the composites (A-E) is shown in Fig. 5. All the composites exhibit better wear resistance compared to that of the base alloy. Al-Si-Mg alloy shows higher wear rate up to a sliding distance of about 1000 m and a gradual decrease thereafter. This is due to the strain hardening of the alloy on increasing the sliding distance[15].

From the graph it can be seen that the composites exhibits two different stages of wear rate behaviour. During the first stage, all composites exhibit increase in wear rate up to a sliding distance of about 1000 m. In the second stage, after 1000 m, the wear rate exhibits more or less a steady change. The variation in wear rate with sliding distance is due to the change in run in wear condition to steady state. The steady condition is achieved due to the material acquiring constant temperature between the sample surface and the steel disk surface. This is due to the fluctuations in wear rate during the initial stage of sliding[4].

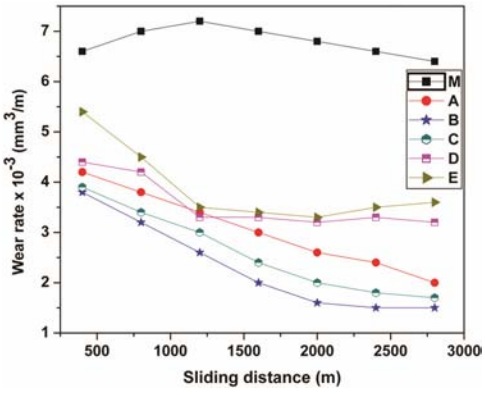

Fig. 5 – Wear rate vs sliding distance at 15 N load for base alloy (M) and composites (A-E)

Composite B showed the best wear resistance with lowest wear rate. Next to composite B, composite C showed good wear resistance. The reason may be due to the strong interfacial bonding rendered by the zircon particles and high hardness rendered by the alumina particles. Refinement in matrix microstructure is also attributed towards the increased wear resistance in the case of both the composites.

Composite A and composite E has higher wear rate due to the clustering of reinforcement particles. On comparing both the composites, composite A exhibits lower wear rate than composite E due to the presence of higher proportion of harder alumina particles. Even though composite D contains both the reinforcement particles, lesser proportion of harder alumina particles leads to more wear loss during sliding and so there exists a higher wear rate for composite D.

Morphological analysis of worn surface

Figure 6(a) shows the worn surface of Al-Si-Mg alloy, and the material loss is found to be very high along the sliding direction. Figures 6(b) and 6(f) show respectively the worn surface of composite A and composite E. Both the micrographs reveal the formation of deeper abrasive grooves along the sliding direction leading to more material loss. Clustering of reinforcement particles in both the composites leads to pull out of particles from the matrix and can be observed from the micrographs. Pulled out particles may get trapped between the pin and the disc further increasing the material loss by ploughing action.

Figure 6(c) shows the worn surface of composite B and the SEM image reveals smooth surface with formation of shallow abrasive grooves along sliding direction indicating less material loss. Figures 6(d) and 6(e) show the worn surface of composite C and composite D respectively. Micrographs reveal the formation of deep abrasive grooves running along the sliding direction forming a delaminated surface. SEM image of the worn surface of composite D (Fig. 6(e)) reveals the debonding of alumina particles leading to particle pull out from the matrix.

In the worn surface micrograph of all the synthesized composites, there is no evidence of plastic deformation of matrix phase. Abrasive wear mechanism and particle pull out is the common feature observed from all the composites.

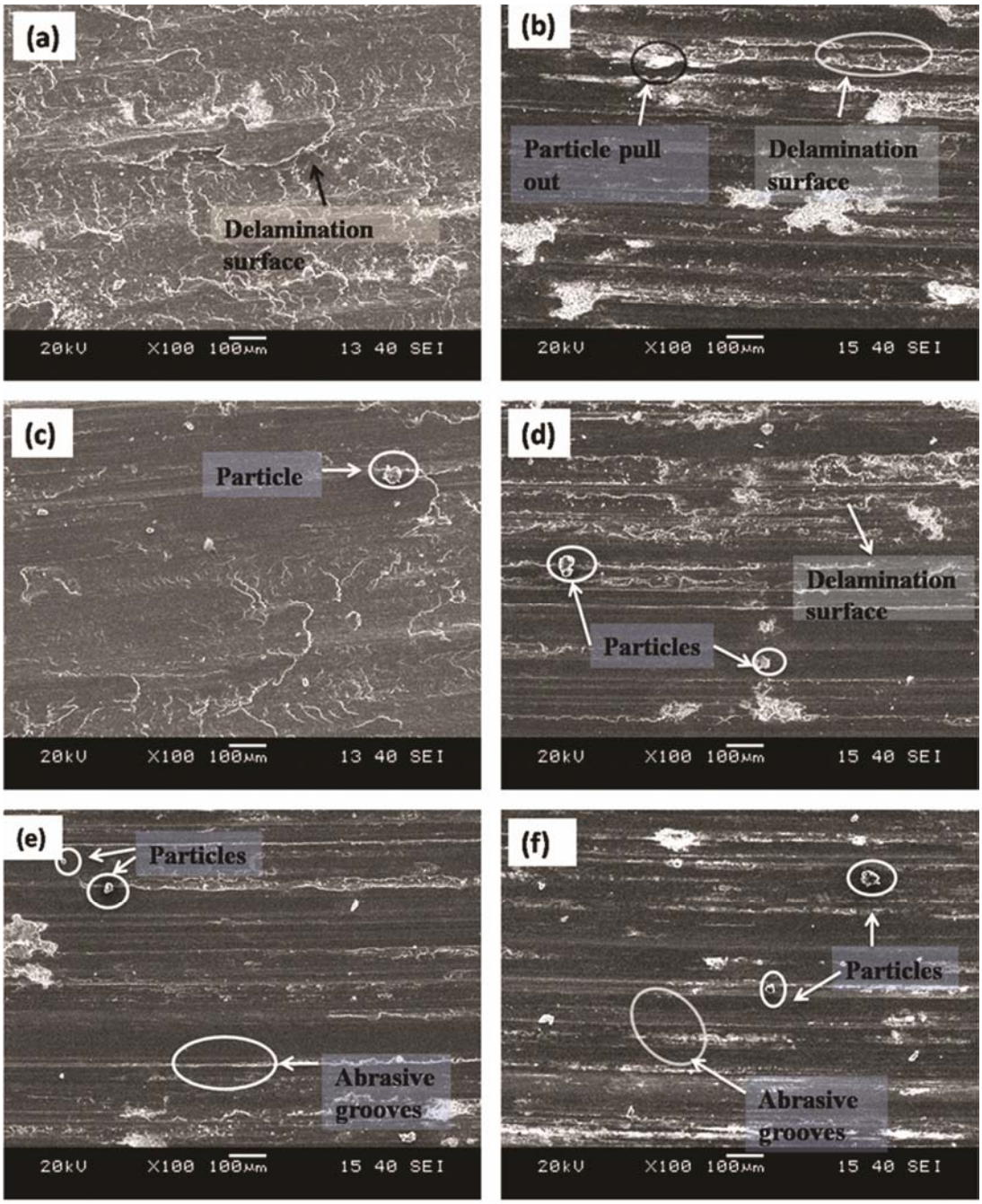

Fig. 6 – SEM images of wear track at a test load of 15N (a) Al-Si-Mg alloy (b) Composite A (c) Composite B (d) Composite C (e) Composite D (f) Composite E

Conclusions

In the present work, the effect of zircon and alumina reinforcement in Al-Si-Mg alloy was studied by incorporating different wt% of reinforcing particles into the alloy limiting the total wt% to 15. Microstructure of the synthesised hybrid composites revealed a uniform distribution of the reinforcement particles. Composite B exhibited better hardness and wear resistance compared to all other composites. This can be attributed to the strong bonding rendered by zircon particles as well as due to high hardness of alumina particles. SEM analysis of worn surface of hybrid composites shows no evidence of plastic deformation of matrix phase. Abrasive wear mechanism and particle pull out is the common feature observed from all the composites.

Acknowledgments

The authors would like to thank the management and the Principal, PSG College of Technology, for providing funds and facilities to carry out the research work.

References

1 Das S, Udhayabanu V, Das S & Das K, ***J Mater Sci,*** 41 (2006) 4668-4677.
2 Das S, Das K & Das S, ***J Compos Mater***, 43 (2009) 22-25.
3 Kumar S, Panwar R S & Pandey O P, ***Ceram Int,*** 39 (2013) 6333-6342.
4 Panwar R S, Kumar S, Pandey R & Pandey O P, ***Tribol Lett***, (2014). DOI 10.1007/s11249-014-0335-y.
5 Gopi K R, Mohandas K N, Reddappa H N & Ramesh M R, ***Int J Eng Adv Technol,*** 2 (2013) 340-344.
6 Sharma V, Kumar S, Panwar R S & Pandey O P, ***J Mater Sci,*** 47 (2012) 6633-6646.
7 Guo M L T & Tsao C Y A, ***Compos Sci Technol***, 60 (2000) 65-74.
8 Wang Y Q, Afsar A M, Jang J H, Han K S & Song J I, ***Wear,*** 26 (2010) 8863-8870.
9 Ahlatci H, Kocer T, Candan E & Cimenoglu H, ***Tribol Int,*** 39 (2006) 213-220.
10 Song J I, Bong H D & Han K S, ***Scr Metall Mater,*** 33(1995) 1307-1313.
11 Kumar S, Sharma V, Panwar R S & Pandey O P, ***Tribol Lett,*** 47 (2012) 231-251.
12 Hashim J, ***J Teknol***, 35 (2006) 9-20.
13 Chaudhury S K, Singh A K, Sivarama Krishnan C S & Panigrahi S C, ***Wear***, 25 (2005) 8759-8767.
14 Okafor E G & Aigbodion V S, ***Tribol Indus,*** 32 (2010) 31-37.
15 Arsenault RJ & Shi N, ***Mater Sci Eng,*** 81 (1986) 175-187.
16 Mrowka-Nowotnik G, Sieniawski J & Wierzbinska M, ***J Achiev Mater Manuf Eng,*** 20 (2007) 155-158.
17 Kumar S, Panwar R S & Pandey O P, ***Ceram Int,*** 39 (2013) 6333-6342.
18 Kumar Suresh, Sharma Vipin, Panwar R S & Pandey O P, ***Tribol Lett,*** 47 (2012) 231-251.
19 Panwar R S & Pandey O P, ***Mater Charact,*** 75 (2013) 200-213.
20 Lashgari H R, Zangeneh Sh, Shahmir H, Saghafi M & Emamy M, ***Mater Des,*** 31(2010) 4414-4422.
21 Aigbodion V S, ***J King Saud Univ–Eng Sci,*** 26 (2014) 144-151.